

Article

Iron Extraction from South African Ilmenite Concentrate Leaching by Hydrochloric Acid (HCl) in the Presence of Reductant (Metallic Fe) and Additive (MgSO₄)

Khetho Daba¹, Munyadziwa Mercy Ramakokovhu¹ , Tajudeen Mojisola^{2,3} , Mxolisi Brendon Shongwe¹ and Nthabiseng Ntholeng^{1,*} 

¹ Department of Chemical, Metallurgical and Materials Engineering, Tshwane University of Technology, Pretoria 0001, South Africa

² Centre for Nano-Engineering and Tribocorrosion, School of Mining, Metallurgy and Chemical Engineering, University of Johannesburg, Johannesburg 2006, South Africa

³ Department of Metallurgical and Materials Engineering, Air Force Institute of Technology, Kaduna 800283, Nigeria

* Correspondence: sthabi@gmail.com; Tel.: +27-12-382-4858

Abstract: The high content of iron in ilmenite ore poses a great challenge, particularly in the synthesis of titanium-containing products due to high susceptibility of iron (Fe) to corrosion. Direct leaching of ilmenite ore in hydrochloric acid (HCl) encouraging Fe dissolution was investigated. The influence of variable parameters, the use of additives, and the addition of metallic iron powder were studied to establish the optimum leaching parameters. The results showed that ilmenite with the particle size distribution of +150 μm yielded better efficiencies when leaching was performed with an acid concentration of 7.5 M and a solid-to-acid ratio of 1:10 at 90 °C. An agitation speed of 450 rpm yielded a superior Fe extraction of about 92.32% and a 2.40% titanium (Ti) loss. The addition of both metallic Fe and the MgSO₄ additive significantly enhanced Fe dissolution and decreased Ti recovery in a leach solution. It was found that leaching under optimum conditions produced a solid residue with 1.37% Fe impurity while 98.63% was extracted. The leached residue was comprised of 91.4% TiO₂ rutile phase and contained a high content of the ilmenite FeTiO₃ (4.37%) and SiO₂ (2.23%) impurities, while Al₂O₃, MgO, MnO₂, CaO, V₂O₅, MnO₂, and Cr₂O₃ were below 0.13%. The high TiO₂ content in the leached residue makes it suitable for use as feed in the production of synthetic rutile. The leaching kinetics of Fe dissolution was found to conform to the shrinking core model, where diffusion through the product layer is rate controlling. The calculated activation energy according to the Arrhenius equation was 19.13 kJ/mol.

Keywords: ilmenite concentrate; leaching; additives; reductant; iron (Fe); titanium dioxide (TiO₂)



Citation: Daba, K.; Ramakokovhu, M.M.; Mojisola, T.; Shongwe, M.B.; Ntholeng, N. Iron Extraction from South African Ilmenite Concentrate Leaching by Hydrochloric Acid (HCl) in the Presence of Reductant (Metallic Fe) and Additive (MgSO₄). *Minerals* **2022**, *12*, 1336. <https://doi.org/10.3390/min12101336>

Academic Editor: Wengang Liu

Received: 5 September 2022

Accepted: 19 October 2022

Published: 21 October 2022

Publisher's Note: MDPI stays neutral with regard to jurisdictional claims in published maps and institutional affiliations.



Copyright: © 2022 by the authors. Licensee MDPI, Basel, Switzerland. This article is an open access article distributed under the terms and conditions of the Creative Commons Attribution (CC BY) license (<https://creativecommons.org/licenses/by/4.0/>).

1. Introduction

The vast applications of TiO₂ in numerous fields such as the manufacture of pigments in paints, coatings, plastics [1], pharmaceuticals [2], photovoltaic cells [3], the anode material of lithium-ion batteries [4], roofing granules, and the production of titanium alloys for the aerospace industry [5], as well as other industries, has led to the depletion of natural rutile (90%–95% TiO₂). The ever-increasing demand for TiO₂ in various industrial applications has prompted researchers to explore other sources of TiO₂. Although the literature has extensively expounded on the chemical synthesis of TiO₂, it has been proven to be expensive compared to the synthesis from ore deposits, particularly ilmenite [6]. Ilmenite deposits are typically found in beach sands and the major global reserves are in Australia (eastern and western coast), South Africa (Richards Bay), America (eastern coast), India (Kerala), and Brazil (eastern and southern coast) [6]. Apart from being abundant globally, ilmenite has the important advantage of being relatively cheap and beneficial in the manufacturing of Ti- and Fe-based products. The ilmenite composition varies depending on

the location it is found, but it mainly contains both non-metallic compounds and traces of metals [7–9]. The presence of impurities in the ilmenite has been reported to be beneficial in enhancing the activity of Ti-based photocatalysts [6], while others have said it depreciates the market value of ilmenite [10,11]. Previously, hydrometallurgical and pyrometallurgical processes have been employed in the recovery of TiO_2 from ilmenite [12–15]. However, pyrometallurgical processes proved to be commercially expensive due to the high energy requirements (up to 1650 °C) [16–18]. In contrast, hydrometallurgical processing is considerably cheaper, as it can be carried out under a normal atmosphere or pressure [19]. The extraction with acid is deemed beneficial, as it allows for the precise control of the particle shape, size distribution, and crystallinity of the final product through the manipulation of the reaction parameters such as temperature, time, solvent, and surfactant type [17,20]. Above all, the hydrochloric acid leaching process is preferred to other acids, owing to its exceptional ability to efficiently remove impurities, producing high-quality rutile (up to 96%), accelerated leaching, and acid-regeneration technology [21]. Likewise, metal ion recovery in hydrochloric acid solutions is noticeably easier than in the sulphuric acid solutions [22–24]. For example, Sasikumar et al. [24] observed a 96% and 84% Fe recovery in 9.2 M HCl and H_2SO_4 , respectively, at 120 °C after 4 h. Mackay et al. [25] illustrated that ilmenite modification caused by weathering can bring about variation in the reactivity of ilmenite towards hydrochloric acid. This is supported by the fact that ilmenite deposits are mainly found as a mixture of both unaltered and altered, with variation in the composition even if it is found in the same location. Hence, the current study investigates direct acid leaching of South African ilmenite in HCl.

To attain high titanium recovery (98.0%) from ilmenite in hydrochloric acid (4 M), processes such as mechanical activation (ball milling for 90 h) and carbothermic reduction (using activated carbon as reducing agent and annealing temperature of 1000 °C) have been developed [26,27]. Mechanical activation enhances the dissolution rate through surface modification and the generated structural defects and strain [28–31]. On the other hand, carbothermic reduction is mainly employed to reduce iron to allow the easy removal of Fe. However, it was discovered that the oxidation performed before reduction at a high temperature yields hematite. The produced ferric iron after oxidation is rather difficult to dissolve. Mahmoud et al. [9] explored a different approach to reducing iron by adding metallic Fe powder to the HCl solution. The study revealed that, indeed, the added metallic Fe acted as a reducing agent and was it suitable, as it did not introduce impurities in the system. Apart from reducing Fe, it was found that introducing additives such as phosphates, fluorides, chlorides, etc., enhanced the leaching of ilmenite. For example, Das et al. [32] carried out ilmenite leaching with hydrochloric acid in the presence of various chloride salts and found CaCl_2 to be more effective due to its higher solubility. Gireesh et al. [33] reported the catalytic effect of sulphate ion. Habib et al. [34] illustrated that a small addition of methanol enhanced the dissolution of ilmenite in HCl. Hence, the current study seeks to explore the effect of fluorides, phosphates, and sulphate ions in Fe dissolution and the viability of the process for industrial application.

In this study, the direct leaching of ilmenite in hydrochloric acid was investigated to establish the dissolution of Fe. The optimization of the leaching conditions was established by studying the leaching parameters, such as particle size distribution, acid concentration, leaching time, agitation, temperature, and solid–liquid ratio. The influence of the reducing agent (iron metallic powder) and use of additives on the leachability of Fe was explored. Moreover, the leaching efficiency of Fe was investigated using magnesium sulphate (MgSO_4), sodium fluoride (NaF), and trisodium phosphate fertilizer (Na_3PO_4) to demonstrate the catalytic effect of monovalent (Na) and divalent (Mg) metal ions. Thereafter, the mechanism of leaching kinetics under various conditions was determined.

2. Materials and Methods

2.1. Materials

The ilmenite beach placer sands ore was provided by Richards Bay Minerals in South Africa. The as-received ilmenite was homogeneously mixed and split before attaining a representative sample for analyses. Thereafter, the ilmenite ore was sieved with standard laboratory Tyler series sieves with different screen sizes to obtain -75 , $+106$, and $+150$ μm , and particle size distribution was confirmed by the Malvern particle size analyzer (Malvern Panalytical (Pty) Ltd., Johannesburg, South Africa). After sieving, 10 g from each size fraction was subjected to elemental analysis to give the composition of the bulk ore.

2.2. Characterization

Phase identification of the ilmenite ore was carried out using the X-ray diffractometry (PANalytical X'Pert Pro powder diffractometer, Almelo, The Netherlands) with Cu- $K\alpha$ radiation ($\lambda = 1.5406$ A) recorded from 5° to 90° with a step size of 0.02° . Chemical composition was determined by X-ray fluorescence (Thermo Fisher ARL Perform X, XRF spectrometer, Thermo Fisher Scientific Inc., Madison, WI, USA) at 4 KV, using IQ⁺ "standard less analysis". The ore was digested in an aqua regia solution consisting of different ratio amounts of HNO_3 and HCl to examine elemental composition with ICP-OES (inductively coupled plasma–optical emission spectrometry, V710, Varian Inc, Yarnton, UK). Grain morphology of the concentrate was studied with scanning electron microscopy (SEM) (model JSM 7600F, JEOL, Akishima, Japan) and the elemental distribution was investigated with energy dispersive spectrometry (EDS model JSM 7600F, JEOL, Akishima, Japan).

2.3. Leaching Experiments

Direct leaching of ilmenite concentrate was performed in a 250 mL glass reactor fitted with a mechanical stirrer. The reactor was heated using a hot plate while the slurry was agitated with a mechanical stirrer. The pH meter with a temperature gauge was used to measure both temperature and the pH. Analytical high-grade HCl and deionized water were used to prepare the solutions. The prepared acid solutions with the required concentrations were preheated to the desired temperature. Thereafter, 70 g of ilmenite concentrate was transferred into the reactor and the agitation was switched on immediately. The leaching experiment was carried out over a period of 60 min. During this time, 15 mL of pregnant leach solution was extracted from the reactor using a syringe at 15 min intervals until the leaching cycle was complete. The extracted pregnant leach solution diluted with deionized water was characterized using ICP-OES (inductively coupled plasma–optical emission spectrometry) to determine the leaching efficiency based on the amount of iron removed from the ilmenite. The leaching efficiency was calculated using Equation (1): where R (%) is the recovery of Fe and M is mass in grams.

$$R (\%) = \left(\frac{M_{\text{Fe removed}}}{M_{\text{Fe in ilmenite}}} \right) \times 100 \quad (1)$$

Metallic iron powder (4.5–6.5 g) was used as a reducing agent while MgSO_4 (10–40 g), Na_3PO_4 (30 g), and NaF (30 g) were added as additives to induce the catalytic effect and reduce the quantity of the free acid and fines produced in a leach solution. Various parameters, such as temperature, acid concentration, agitation, solid-to-liquid ratio, and retention time, were studied to optimize the leaching conditions. The mechanism of leaching kinetics was proposed based on the optimized conditions. The leaching conditions are shown below in Table 1.

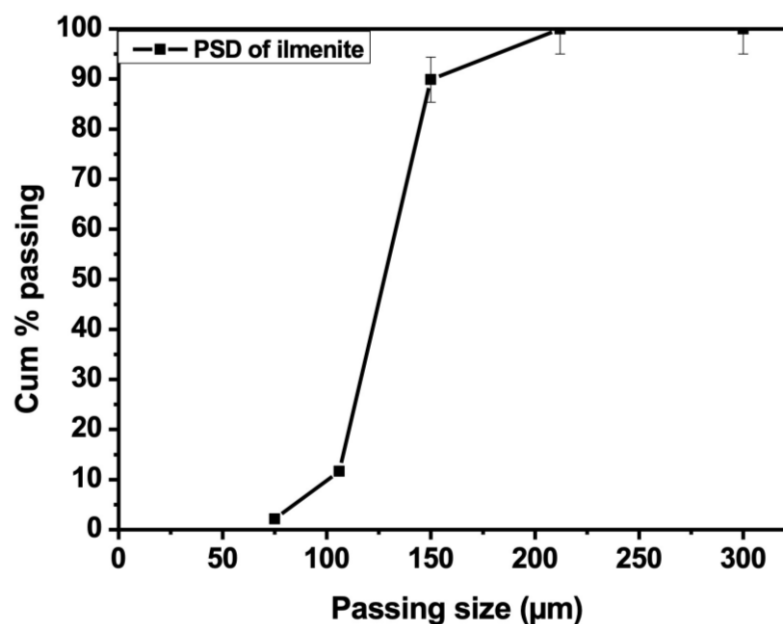
Table 1. Experimental leaching conditions.

Leaching Experiment	Material	Temperature (°C)	Concentration (M)	Additives (30 g)
Condition 1	70 g ilmenite HCl	70	2.5	
		80	5	
		90	7.5	
Condition 2	70 g ilmenite HCl	90	7.5	Fe metallic powder MgSO ₄ Na ₃ PO ₄ NaF

3. Results and Discussion

3.1. Mineralogical Analysis

The particle size distribution (PSD) of the as-received ilmenite ore was measured with Malvern, and the results are shown in Figure 1. The particle size ranged from 75 to 300 μm . The ilmenite ore consists of particles with a d_{50} of around 129 μm , while the d_{10} and d_{90} is 98 μm and 150 μm , respectively.

**Figure 1.** Particle size distribution of the as-received ilmenite ore.

Compositional analysis of the raw ilmenite was conducted on various fraction sizes. The X-ray fluorescence results are shown in Table 2 below. The obtained results depict that iron and titanium in the ilmenite ore are present as the hematite and rutile, respectively. The ore contains a high amount of Fe_2O_3 of about 48.23% and 42.93% of TiO_2 . The formation of the hematite phase indicates gradual weathering. The ore contains high Al_2O_3 , SiO_2 , and MnO impurities compared to others, which are available in less than 1%, indicating alteration in the ore. However, it is noticed that the ore with a particle size of $-75 \mu\text{m}$ and $+150 \mu\text{m}$ have a high SiO_2 content of about 4.63% and 5.61%, respectively, suggesting that they may be resistant to leaching in HCl [35].

After sieving the ilmenite ore into various fraction sizes, morphological analysis was carried out on the powdered samples ($+75 \mu\text{m}$ and $+106 \mu\text{m}$) mounted on the aluminium stub using conductive two-sided tape. The obtained SEM images are presented in Figure 2. Morphology examination of the concentrate shows a mixture of elongated, semi rhombohedral, and subrounded grains (Figure 2a). The sphericity of the particles ranges from low to medium. Zooming into the particle surface formation of cracks and pits (Figure 2b) is

evident, which may be beneficial in the fast penetration of the acid solution into the material. The formed cracks could be due to repeated particle collision during transportation, while it is suspected that the brittle fracture may have induced physical deformation resulting in the diversity in the grain morphology. Ramakokovhu et al. [36] suggested that pits could be due to the migration of atoms from crystalline structures, causing alteration in the mineral. Apart from Ti and Fe, traces of impurities such as Al, Si, P, Ca, and Mn (Figure 2c) are detected by EDS. Similarly, Mojisola et al. [37] observed the same impurities on the ilmenite structure. However, variation in the impurities may arise due to the weathering process which occurs over time. The formation of Al and Si impurities indicates the occurrence of post-depositional weathering in the sedimentary and laterites. Additionally, Al and Si impurities are detected on the grain surface (Figure 2d) compared to P, Ca, and Mn, which were not detected. This suggests that P, Ca, and Mn impurities could be trapped in between the FeTiO₃ grains. Klepka et al. [38] and Nayl and Aly [39] reported that, if impurities are trapped in FeTiO₃ grains, their oxide is attached to the boundaries of the large grains.

Table 2. Chemical analysis of the ilmenite ore with various sizes.

Compounds	Percentage (wt.%)				
	Ilmenite	−75 μm	+75 μm	+106 μm	+150 μm
Fe ₂ O ₃	48.23	46.49	48.10	48.39	47.20
TiO ₂	42.93	41.47	43.55	43.34	39.99
SiO ₂	2.94	4.63	2.49	2.51	5.61
Al ₂ O ₃	1.71	2.17	1.63	1.65	2.21
MnO	1.11	1.04	0.99	1.06	1.36
MgO	0.80	1.08	0.84	0.81	0.90
V ₂ O ₅	0.39	0.40	0.42	0.40	0.33
Cr ₂ O ₃	0.17	0.35	0.24	0.14	0.40
ZrO ₂	0.16	0.34	0.22	0.12	0.09
CaO	0.13	0.43	0.12	0.11	0.24
Na ₂ O	0.13	0.15	0.11	0.18	0.29
Nb ₂ O ₅	0.19	0.14	0.09	0.1	0.59
P ₂ O ₅	0.15	0.16	0.06	0.06	0.43
Co ₃ O ₄	0.13	0.14	0.08	0.04	0.07
K ₂ O	0.16	0.09	0.05	0.05	0.09
ZnO	0.14	0.07	0.09	0.07	0.05
Gd ₂ O ₃	0.10	0.01	0.02	0.02	0.01
LOI	0.43	0.84	0.9	0.95	0.14
Total	100	100	100	100	100

LOI = loss on ignition.

The ICP analysis was performed to quantify the elemental composition of the ilmenite ore. Digestion of the concentrate (10 g) was carried out in an aqua regia solution (100 mL) at a temperature of 110 °C for 2 h. The dissolution behaviour of the ilmenite was investigated with an aqua regia solution consisting of various concentrations. The dissolved amounts of metal ions are shown in Figure S1, and the elemental percentages of the major elements are illustrated in Table 3. As shown in Figure S1, the dissolution behaviour of both major and trace elements improves with an increase in the aqua regia concentration, resulting in high amounts of dissolved metal ions. Moreover, it is observed that Fe dissolution significantly increased from 130 mg/L (Figure S1a) to 40.55 mg/L (Figure S1c), corresponding to 53.3% and 79.9% (Table 3), respectively. This suggests that the high acid concentration may be effective in achieving a high Fe dissolution. However, Ti recovery is low compared to Fe, contradicting the stoichiometric ratio of Fe and Ti shown by XRF (Table 2). Similarly, Haverkamp et al. [40] observed low Ti recovery in HCl between 85 and 90 °C. The decrease in Ti digestion was attributed to hydrolysis and the precipitation of the TiO(OH)₂. The TiO(OH)₂ precipitates tend to coat the ilmenite surface or block the pores, preventing further digestion. Vilakazi et al. [41] observed a similar trend in HCl, HNO₃, and aqua regia solutions. Therefore, it is anticipated that the Ti recovery will be low in the leach

solution. According to the results illustrated in Table 3, Fe, Ni, S, Cu, Al, and C are the major detected elements while Si, Zn, and Th are considered minor elements, as they are available in minute percentages. The presence of La and Co elements is related to the formation of the pseudorutile phase [42].

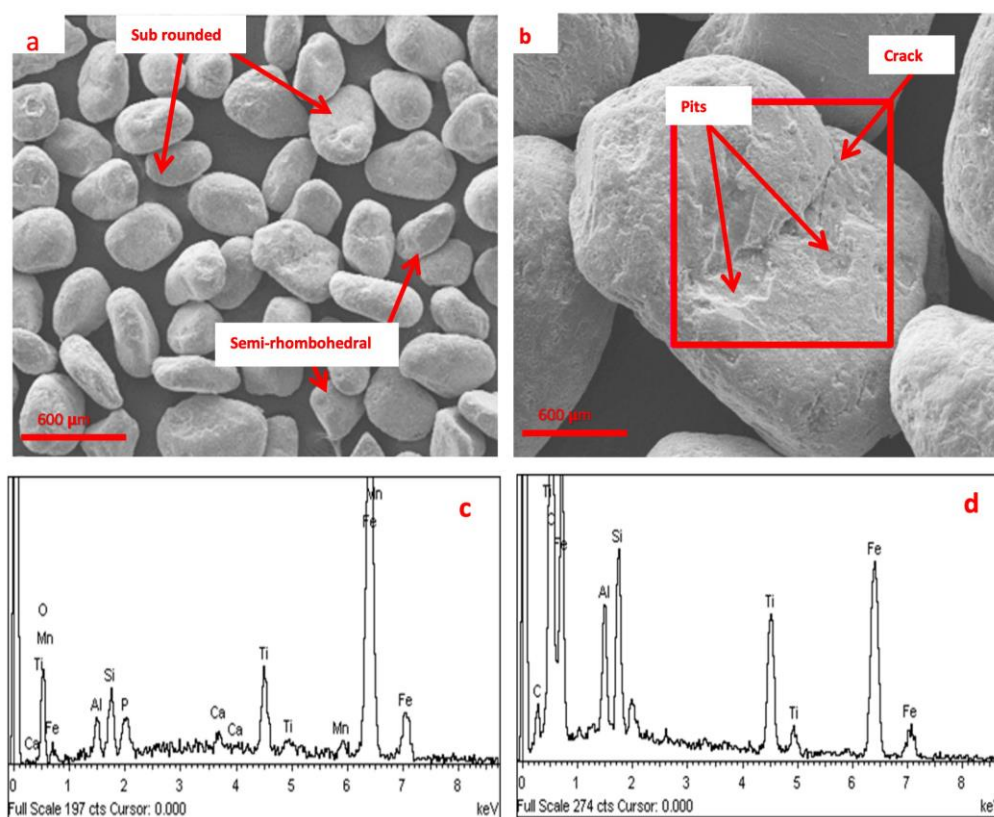


Figure 2. SEM micrograph of ilmenite with particles sizes of (a) +75 µm and (b) +106 µm and EDS analysis of sizes (c) +75 µm and (d) +106 µm.

Table 3. Elemental analysis of the ilmenite ore by ICP-OES (wt%).

Elements	Concentration	
	10 mL HNO ₃ 30 mL HCl	20 mL HNO ₃ 60 mL HCl
	wt%	wt%
Al	9.1	6.4
Co	12.7	2.3
Cu	4.5	1.2
Fe	53.3	79.9
Ni	12.3	7.1
S	4.9	1.6
Si	0.8	0.4
* Zn	0.6	-
* Th	-	0.1
Ti	0.1	0.1
Other impurities	1.7	0.9

* wt.% included in other impurities.

The crystal structure of the raw ilmenite was investigated by X-ray diffraction analysis. The X-ray diffraction pattern is shown in Figure 3. According to the obtained results, ilmenite FeTiO₃ (PCPDFWIN#:00-071-1140), rutile TiO₂ (00-075-1757), pseudorutile Fe₂Ti₃O₉ (00-41-1777), and silica SiO₂ (00-082-0511) are the detected phases. The ilmenite (FeTiO₃) appears to be the most prominent phase, which is consistent with the high amounts of

Fe_2O_3 detected by XRF (Table 2). However, the observed TiO_2 phase contradicts the XRF measurements (Table 2), which exhibited close to 50-50 split of Fe and Ti. This could be attributed to the presence of Al_2O_3 and SiO_2 , which enable impurity inclusions within the structure post-deposition [36]. In addition, the presence of the pseudorutile phase accounts for the inconsistent Ti amounts. The diffraction peaks of the $-75 \mu\text{m}$ and $+150 \mu\text{m}$ are broad and have low intensity compared to $+75 \mu\text{m}$ and $+106 \mu\text{m}$, indicating low crystallinity. Moreover, SiO_2 impurity was not detected in the other samples, except on the concentrate with a high particle size range of $+106 \mu\text{m}$. Since the Cr, V, Al, and Ca impurities were not detected by XRD, it implies that the impurities may have substituted Fe atoms in the crystal structure of FeTiO_3 and are trapped as small grains in-between the ilmenite phases. Hugo et al. [43] elaborated that variation in the chemical composition of ilmenite typically occurs as Mg^{2+} , Mn^{2+} , and Fe^{3+} substitute the Fe^{2+} in the crystal structure. According to the XRD and XRF results, different Fe phases were detected; therefore, it can be assumed that cation substitution may have taken place. The formation of the $\text{Fe}_2\text{Ti}_3\text{O}_9$ phase is associated with the presence of La and Co elements in the ore, which was confirmed by ICP measurements (Figure S1) [42].

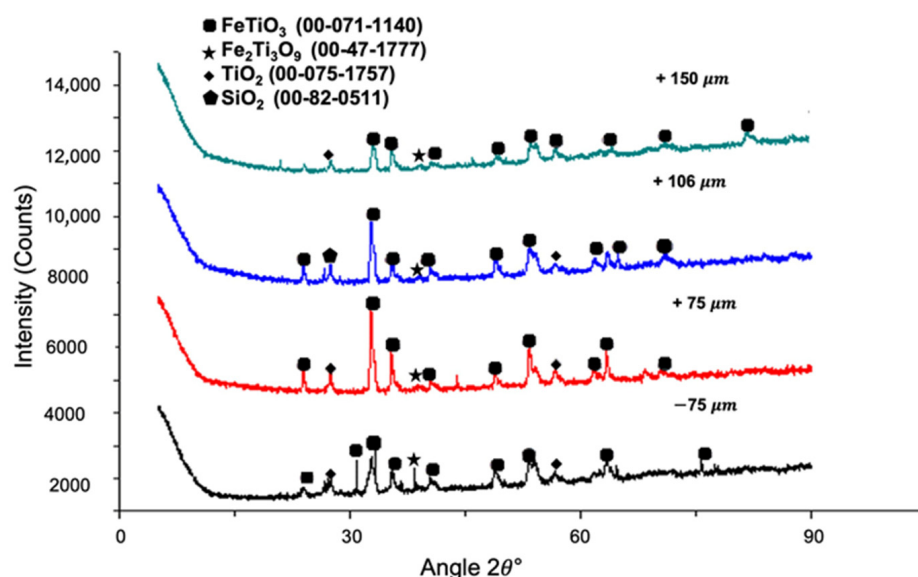
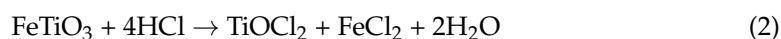


Figure 3. XRD patterns of the as-received ilmenite ore with various particle size distributions.

3.2. The Effect of Particle Size Distribution

The leaching behaviour of the ilmenite ore with various fraction sizes was investigated using the acid-to-ilmenite ratio of 10:1 with 7.5 M HCl at 90 °C for 60 min. The agitation speed was kept at 350 rpm during the entire duration of the leaching process. The extraction of Fe from the samples as a function of time is illustrated in Figure 4. The overall reaction for the dissolution of ilmenite in hydrochloric acid occurs according to reaction (2), while hematite dissolution follows reaction (3).



As the reaction (1) progresses, hydrolysis takes place, generating HCl, as described by reaction (4).



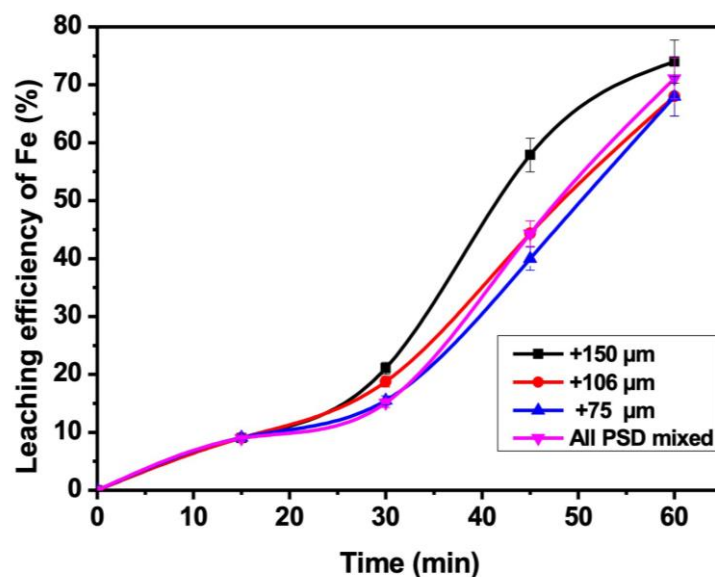


Figure 4. The effect of particle size distribution on leaching efficiency of Fe. Conditions: 7.5 M HCl; solid–liquid ratio, 1:10; agitation speed, 350 rpm; agitation time, 60 min; temperature, 90 °C.

The dissolution of Fe in HCl is particle-size-dependent, as it increases with an increasing particle size. The highest Fe removal of 74% was achieved with a fraction size of +150 μm, while both +75 μm and +106 μm showed an efficiency of less than 70%. This contradicts the findings of Olanipekun et al. [44], who reported that finer particles (20–37 μm) exhibited the highest Fe dissolution in 7.2 M HCl at 70 °C. Furthermore, numerous studies have shown that particle size reduction induced via mechanical milling tends to enhance the dissolution rate due to the increased surface area and crystal structure deformation [24,45]. The crystal structure deformation weakens the bonds, leading to a rapid reaction rate. In the current study, the decreased dissolution rate observed with small-sized particles could be attributed to their high susceptibility to weathering, resulting in high silicate and alumina impurities (Table 2), which tends to reduce the Fe: Ti ratio in the feed. Similarly, Jabit et al. [46] observed a low dissolution rate with altered ilmenite with small-sized particles. The low dissolution rate of Fe was ascribed to the formation of the pseudorutile ($\text{Fe}_2\text{Ti}_3\text{O}_9$) phase, which slowed down the reaction due to the stability of the Ti-O bond. Moreover, the pseudorutile ($\text{Fe}_2\text{Ti}_3\text{O}_9$) is made up of 1:5 mole ratio of Ti:Fe, which is known to have a lower reactivity than unaltered ilmenite. Therefore, since the $\text{Fe}_2\text{Ti}_3\text{O}_9$ phase is detected, it cannot be ruled out that the Fe^{2+} substitution in the lattice structure may have occurred with elements such as Ca^{2+} , Mn^{2+} , and Fe^{3+} [47]. Moreover, manganese in the range of 0.6%–1% is favourable to the weathering transformation phase (pseudorutile) [32]. Since the high efficiency was obtained with +150 μm, it will be taken as the optimum particle size range for this study.

3.3. Influence of HCl Acid Concentration

Since the acid concentration is considered chemical activation in the decomposition of ilmenite, the influence of the acid concentration on iron dissolution was undertaken by varying the concentration between 2.5 M and 7.5 M using ilmenite particles with a fraction size of +150 μm. The solid–liquid ratio was 1:10, while the agitation speed was kept at 350 rpm at a temperature of 80 °C (below the boiling point of HCl 84 °C) for the duration of 60 min. According to the dissolution curves in Figure 5, the Fe extraction from the ore increased consistently with an increase in the acid concentration. For example, at a low concentration of 2.5 M, the maximum Fe leachability is 59%, which increased to 68% by doubling the concentration. The Fe efficiency reaches 76% after 60 min of leaching with 7.5 M HCl. The increase in efficiency is due to the enormous effect of the high acid concentration on the hydrolysis reaction [8]. The high Fe dissolution with 7.5 M HCl was

accompanied by a 1.56% of titanium loss, which is fairly negligible. Therefore, 7.5 M is the optimum concentration that will be employed for further studies.

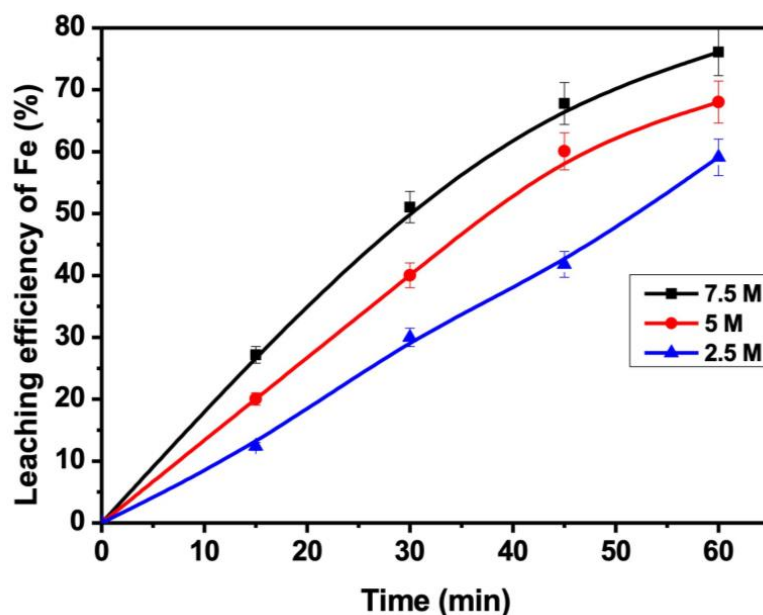


Figure 5. The effect of acid concentration on leaching efficiency of Fe. Conditions: particle size, 150 μm ; solid–liquid ratio, 1:10; agitation speed, 350 rpm; agitation time, 60 min; temperature, 80 $^{\circ}\text{C}$.

3.4. Effect of Temperature

The dependence of temperature on the dissolution rate of Fe and TiO_2 was first noticed by Jackson and Wadsworth [48]. The study showed that the increased leaching temperature resulted in the rapid dissolution of ilmenite. However, it was observed that a high acid-to-ilmenite (692:1.) mole ratio favoured both iron and titanium dissolution into the solution, while Sinha et al. [49] observed mainly iron with a mole ratio of 1:1. For example, Jackson and Wadsworth [48] extracted 100% Fe and Ti at 90 $^{\circ}\text{C}$ after 100 min, while Sinha et al. [49] reported a 95% Fe extraction at 108 $^{\circ}\text{C}$ after 4 h. In a like manner, the influence of temperature on leaching behaviour of Fe was explored. The leaching temperature was varied in the range of 70–90 $^{\circ}\text{C}$ for 60 min, while the acid concentration was kept at 7.5 M, with the slurry consisting of +150 μm ilmenite particles agitated at 350 rpm. The obtained results presented in Figure 6 indicate that the dissolution of Fe from the ore is greatly dependent on the leaching temperature. This could be due to an increase in kinetic energy within the molecule, which tends to promote the breaking of bonds followed by the formation of new bonds. At a moderately low temperature of 70 $^{\circ}\text{C}$, the maximum leachability of Fe reached 63% after 60 min, which is low compared to the 71% obtained at 80 $^{\circ}\text{C}$. A further increase in temperature to 90 $^{\circ}\text{C}$ yielded the maximum Fe extraction of 78% after 60 min. The obtained Fe extraction at 90 $^{\circ}\text{C}$ is low compared to Tao et al. [50], who observed an efficiency higher than 80% and demonstrated that longer leaching times are necessary to obtain higher efficiencies. Therefore, there is an opportunity to obtain a high Fe extraction through the optimization of the leaching time. Moreover, the observed results signify that, at high temperatures and high acid concentrations, Fe-O-Ti bonds are weakened, promoting the dissolution of Fe. This process occurs concurrently with a slight dissolution of TiO_2 due to hydrolysis, which can increase drastically at higher temperatures (>90 $^{\circ}\text{C}$). Again at higher temperatures, the evaporation of HCl tends to occur, resulting in a volatile loss of acid [26]. Based on the achieved results, 90 $^{\circ}\text{C}$ is taken as the optimum leaching temperature for the current study.

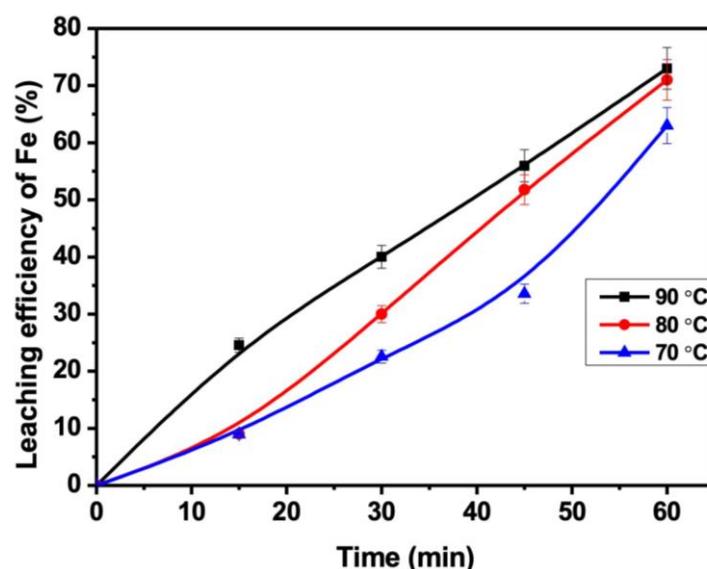


Figure 6. The effect of temperature on the leaching efficiency of Fe. Conditions: particle size, 150 μm ; acid concentration, 7.5 M; solid–liquid ratio, 1:10; agitation speed, 350 rpm; agitation time, 60 min.

3.5. Effect of Agitation Speed

The agitation rate in the ilmenite leaching process is significant, as it ensures that no material settles at the bottom of the leaching vessels, and it increases contact between the solid–liquid phase. The agitation speed was varied between 350 and 550 rpm, while the other parameters were fixed at 90 °C temperature, the solid–liquid ratio of 1:10, and the HCl concentration of 7.5 M with a +150 μm fraction size for the duration of 60 min. Table 4 shows the recovery percentages of Ti and Fe taken at 15 min intervals under various agitation speeds. Generally, it is observed that the recovery percentage increases with the increasing agitation rate, signifying the diffusion of the acid into the surface of the particles [8]. It is observed that there is a heightened recovery of Fe over time, while Ti recovery varies depending on time and speed. Compared to Fe, less Ti is recovered in the solution, indicating that the present leaching process will be beneficial in the rutile synthesis. At a low speed (350 rpm), 40.04% Fe and 2.45% Ti was recovered, which increased to 52.03% and 3.45%, respectively, at 550 rpm. Extending the leaching duration to 60 min significantly improved the Fe dissolution, with the highest recovery of 92.49% recorded at an agitation speed of 550 rpm. Moreover, it is observed that at 550 rpm, there is a high recovery of Ti of 8.35%, which could be ascribed to excessive formation of TiO_2 fines at a high stirring speed [49]. On the other hand, an agitation speed of 450 rpm shows a comparable Fe recovery of 92.32% with a Ti recovery of 2.40%, which is relatively low compared to the 8.35% observed at 550 rpm. Similarly, Ramadan et al. [8] observed high Fe leachability and high TiO_2 precipitates at 400 rpm. Therefore, based on the obtained results, the optimum agitation speed is 450 rpm.

Table 4. Chemical analysis of the ilmenite ore with various sizes (350, 450 and 550 rpm).

Time (min)	350 rpm Actual Recovery		450 rpm Actual Recovery		550 rpm Actual Recovery	
	Fe %	Ti %	Fe %	Ti %	Fe %	Ti %
15	40.04	2.45	50.61	4.40	52.03	3.45
30	58.14	3.08	78.35	4.68	81.65	4.80
45	70.11	2.23	89.45	2.80	90.61	5.33
60	81.99	2.45	92.32	2.40	92.49	8.35

3.6. Effect of Solid–Liquid Ratio

The effect of solid and the liquid ratio was also studied, as it determines whether both Fe and Ti get passed into the solution. The solid–liquid ratios varied between 1:10 and 3:20, and the other parameters were fixed. The dissolution curves in Figure 7 show that, as the solid–liquid ratio increases, the iron dissolution is reduced. According to van Dyk et al. [51], at high acid-to-ilmenite mole ratios, the polymerization reaction tends to slow down, leading to the formation of TiOCl_2 in the leach solution. The formed TiOCl_2 fines precipitate in the pores of the particles, hindering acid diffusion into the particle surface. Based on the obtained results in Figure 7, it is observed that, when the solid-to-liquid ratio is 1:10 and 1:20, almost 92.3% of the Fe is leached out. This indicates that, at a low solid–acid ratio and high temperature, the polymerization reaction occurs rapidly, favouring a high iron dissolution. Furthermore, it has been reported that a low solid–acid ratio can cause a reduction in the hydrogen ion concentration [8,51]. The reduction of hydrogen ion yields $\text{TiO}_2 \cdot \text{H}_2\text{O}$ precipitates as a result of reduced acid concentration and an increased pH, which determine the rate-limiting step according to the diffusion of hydrogen ions to the reaction interface [51]. Although both 1:10 and 1:20 solid–acid ratios showed the highest leaching efficiency, the lowest Ti dissolution of 2.24% was obtained with 1:20, thus making it the optimum ratio.

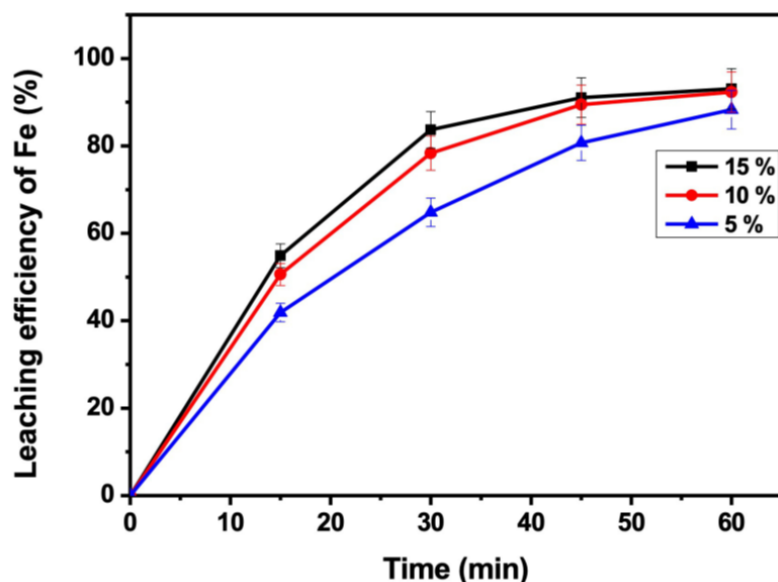
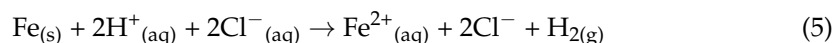


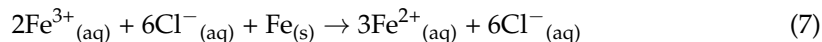
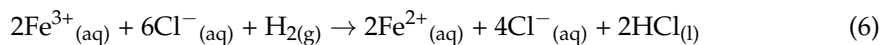
Figure 7. The influence of solid–liquid ratio on Fe dissolution from ilmenite. Conditions: particle size, +150 μm ; acid concentration, 7.5 M; solid–liquid ratio, 1:10, 1:20, and 3:20; agitation speed, 450 rpm; temperature, 90 $^{\circ}\text{C}$; agitation time, 60 min.

3.7. Effect of Metallic Fe Powder Addition

According to the literature reports, the rate of iron leaching in ilmenite is generally improved by the reduction of ferric iron to ferrous iron [9,52]. As reported by Mahmoud et al. [9], iron metal is the best-suited reductant compared to the carbothermic reduction, as it introduces no foreign ions in the reaction medium. During leaching, Fe powder was added to evaluate its influence on Fe extraction. The introduction of Fe into the reaction medium initiates the reaction between HCl and Fe, forming ferrous chloride according to the reaction (5).



The generated H_2 gas will further react with FeCl_3 produced from reaction (5) to reduce Fe^{3+} to Fe^{2+} , as shown in reaction (6), or Fe reduction can occur via reaction (7).



The dependence of Fe extraction on the dosage of the Fe powder is observed in Figure 8. To obtain the correct representative amount of Fe present in the solution, the metallic Fe added was subtracted from the total Fe dissolved. Based on the obtained results, it is observed that the Fe extraction continually increased with an increasing dosage of Fe powder. When leaching was carried out with 6.5 g of the metallic iron dosage, an Fe extraction of 93.39% was achieved after 60 min compared to 76% observed with a minimum dosage of 4.5 g. This could be attributed to a collective effect of the reduction process and the hydration reaction resulting from the high acid concentration. Based on the achieved results, the Fe dosage of 6.5 g will be used in the optimization of the other parameters.

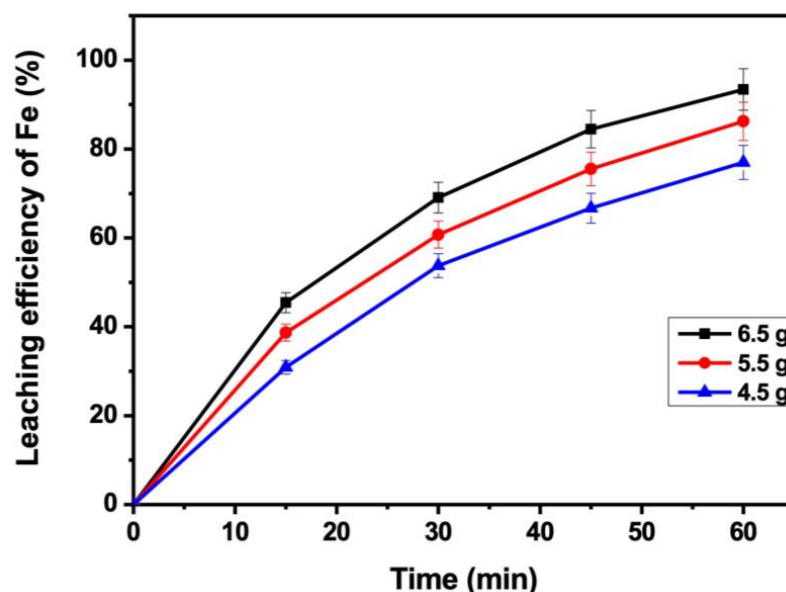


Figure 8. Effect of iron powder addition on the dissolution of Fe. Conditions: particle size, +150 μm ; acid concentration, 7.5 M; solid–liquid ratio, 1:20; agitation speed, 450 rpm; temperature, 90 $^{\circ}\text{C}$; agitation time, 60 min.

3.8. Effect of Additives

Earlier, Reid and Sinha [53] reported the effect of soluble chlorides of FeCl_2 , MnCl_2 , MgCl_2 , NiCl_2 , CaCl_2 , and NH_4Cl_2 on the leaching performance and kinetics. Das et al. [32] illustrated that the addition of CaCl_2 in ilmenite dissolution in hydrochloric acid was more effective compared to MgCl_2 and NaCl . The improvement in the leaching efficiency was due to the high solubility of CaCl_2 and the increased chloride (Cl) concentration. Recently, Gireesh et al. [33] investigated the effect of sulphate ions on the leaching of ilmenite with hydrochloric acid. It was observed that sulphates of divalent metal (Ca and Mg) were superior compared to the sulphates of monovalent metal (Na and K), which showed the lowest dissolution rate. Furthermore, the catalytic effect of sulphate ion lowered the activation energy of the chemical reaction while simultaneously lowering the free-acid content and fine generation. Herein, the extraction of Fe from ilmenite in hydrochloric acid with MgSO_4 , Na_3PO_4 , and NaF additives combined with metallic Fe was investigated. During this time the optimum parameters utilized were 7.5 M HCl, the temperature of 90 $^{\circ}\text{C}$, a solid–liquid ratio of 1:20, the particle size of +150 μm , and an agitation rate of 450 rpm for the duration of 60 min. The maximum iron dissolution of 94.8% was achieved

with MgSO_4 (Figure 9a), which could be due to accelerated iron dissolution through the reduction of ferric iron in the HCl acid solution. The accelerated iron dissolution was achieved by the catalytic action of sulphate ions through the reduction of the energy gap of the chemical reaction [33]. Moreover, the achieved efficiency of 94.8% in the present study is higher than the value reported by Gireesh et al. [33], which was below 94%, but it is close to 95% efficiency, which was achieved with the addition of CaSO_4 , thus proving the efficiency of the currently established leaching conditions. Furthermore, the high efficiency with MgSO_4 was expected, as it has previously been shown that the divalent metal sulphates tend to show superiority in Fe removal compared to monovalent metal sulphates. In comparison to Na_3PO_4 , NaF showed better efficiency, coming second to MgSO_4 . This could be due to high affinity of fluorides for iron and titanium oxide. Dubenko et al. [54] observed that adding NaF in H_2SO_4 leaching of ilmenite formed gaseous HF bubbles yielding holes and recesses on the sample surface. This permits the interface reaction between the ilmenite and bubbles to be controlled by the rate of reaction and diffusion rate of the reagent. The lowest efficiency was obtained with Na_3PO_4 due to low solubility of phosphates ions compared to the rest. The observed result is in agreement with the findings of Duncan and Metson [28], who reported that the addition of bisulphate and fluoride into the leach solutions showed the high dissolution rate of both iron and titanium, while the addition of phosphoric acid drastically decreased the dissolution rate.

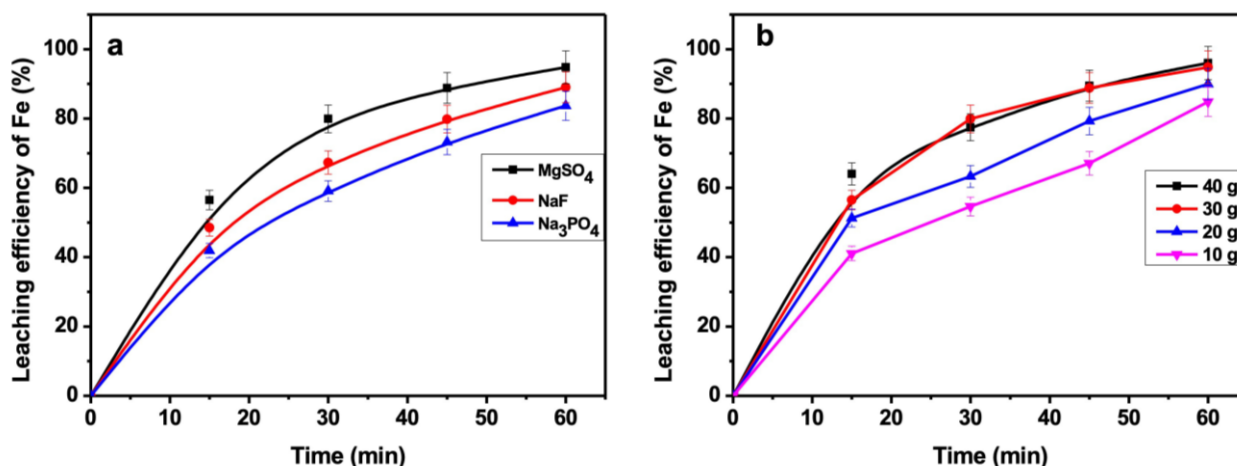


Figure 9. The influence of (a) additives and (b) magnesium sulphate dosage on leaching efficiency of Fe. Conditions: particle size, +150 μm ; acid concentration, 7.5 M; Fe powder, 6.5 g; solid–liquid ratio, 1:20; agitation speed, 450 rpm; temperature, 90 $^{\circ}\text{C}$; agitation time, 60 min.

Since the high Fe dissolution rate was achieved with MgSO_4 , it was taken as the best-performing additive. Upon varying the dosage of MgSO_4 (Figure 9b) from 30 g to 40 g, the dissolution efficiency of Fe increased from 94.8% to 96.02%, while low dosages of 10 g and 20 g yielded an efficiency below 90%. A similar trend was observed by Gireesh et al. [33].

3.9. Effect of Retention Time

After the optimization of the leaching parameters, the leaching period was extended from 60 to 120 min. The effect of the retention time was studied under various conditions, identified as the HCl condition (normal), Fe-HCl (iron conditions), and Fe- MgSO_4 -HCl (additives condition). From the dissolution curves shown in Figure 10, it is noticed that the retention time played a significant role in the dissolution of iron. Under normal conditions, an iron dissolution (Figure 10a) of 76.02% was achieved after leaching for 60 min, which ultimately reached 87.05% after 120 min. The addition of metallic Fe powder escalated Fe extraction to 93.39% and 97.45% after 60 and 90 min, respectively. The continued rapid leaching after 60 min can be ascribed to the occurrence of a hydrolysis reaction in which active HCl is released [49]. A significant improvement is observed with the addition of

MgSO₄, resulting in the iron dissolution of 97.42% after 90 min and 98.63% after 120 min. Ti leaching (Figure 10b) decreased with an increase in the retention time. Under normal and additives conditions, Ti extraction increased rapidly until 60 min, whereafter it decreased drastically. On the contrary, the lowest Ti (1.28%) was recovered after 60 min under Fe conditions. At 120 min, the lowest (2.56%) and the highest (6.27%) Ti were leached under additives and normal conditions, respectively. The final product had 97.3% Ti recovery and only 1.37% iron impurities, which is acceptable in the marketplace. Therefore, the selected optimum retention time was 120 min under additive conditions, amounting to a 98.63% leaching efficiency.

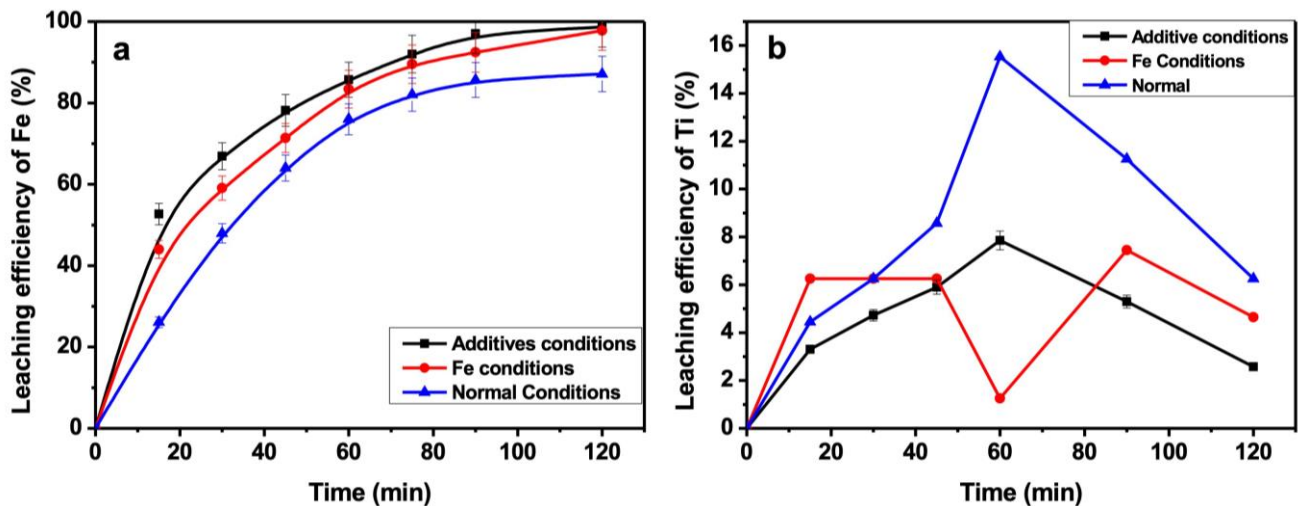


Figure 10. The influence of retention time on the (a) Fe and (b) Ti dissolution under HCl condition (normal), Fe-HCl (iron condition), and Fe-MgSO₄-HCl (additives condition). Conditions: particle size, +150 μm ; acid concentration, 7.5 M; solid-liquid ratio, 1:20; agitation speed, 450 rpm; temperature, 90 $^{\circ}\text{C}$; agitation time, 120 min.

3.10. Leaching Kinetics

Various kinetics models have been reported in the literature to describe the leaching kinetics of the ilmenite ore [8,44]. In the current study, an attempt was made to describe the leaching kinetics of ilmenite via the shrinking core model, in which it is assumed that the ore is a homogeneous spherical solid phase [55]. The Fe dissolution kinetics were investigated using both the product layer diffusion control mechanism and the interfacial chemical reaction mechanism described by Equations (8) and (9), respectively, where x is the fraction of Fe reacted at time t (min) and k_1 ($\text{m}\cdot\text{min}^{-1}$) and k_2 ($\text{m}\cdot\text{min}^{-1}$) are the overall rate constants.

$$1 + 2(1 - x) - 3(1 - x)^{\frac{2}{3}} = k_1 t \quad (8)$$

$$1 - (1 - x)^{\frac{1}{3}} = k_2 t \quad (9)$$

The kinetic Equations (8) and (9) were plotted as a function of reaction time to determine the kinetic parameters under various reaction conditions. The plots of both product layer diffusion control and surface chemical reaction models are shown in Figure 11. The correlation coefficients (R^2) were obtained from the linear straight line, while the rate constants were determined from the slopes of the straight line. The experimental kinetic data obtained according to Equation (8) show high R^2 values compared to Equation (9). Based on the plots obtained from Equation (8) shown below (Figure 11), it is observed that the R^2 varies from 0.993 to 0.936, corresponding to the additive (Fe-MgSO₄-HCl) and normal (HCl) conditions, respectively. This signifies that the predominant dissolution mechanism of ilmenite is controlled by the product layer diffusion, and therefore it is the rate-determining step. Olanipekun et al. [44] demonstrated that, at the temperature range

of 70–90 °C, there are two competing diffusion processes. The Ti^{4+} and Fe^{2+} produced by the surface chemical reaction of the unreacted core compete with the H^+ from HCl. The existence of Ti^{4+} as polynuclear species such as $[(TiO)_8(OH)_{12}]^{4+}$ produces a rather large titanium ion species in the solution compared to H^+ , thus exhibiting a sluggish diffusion [44]. Therefore, the diffusion of Ti^{4+} and Fe^{2+} is considered the rate-controlling step in the dissolution reaction.

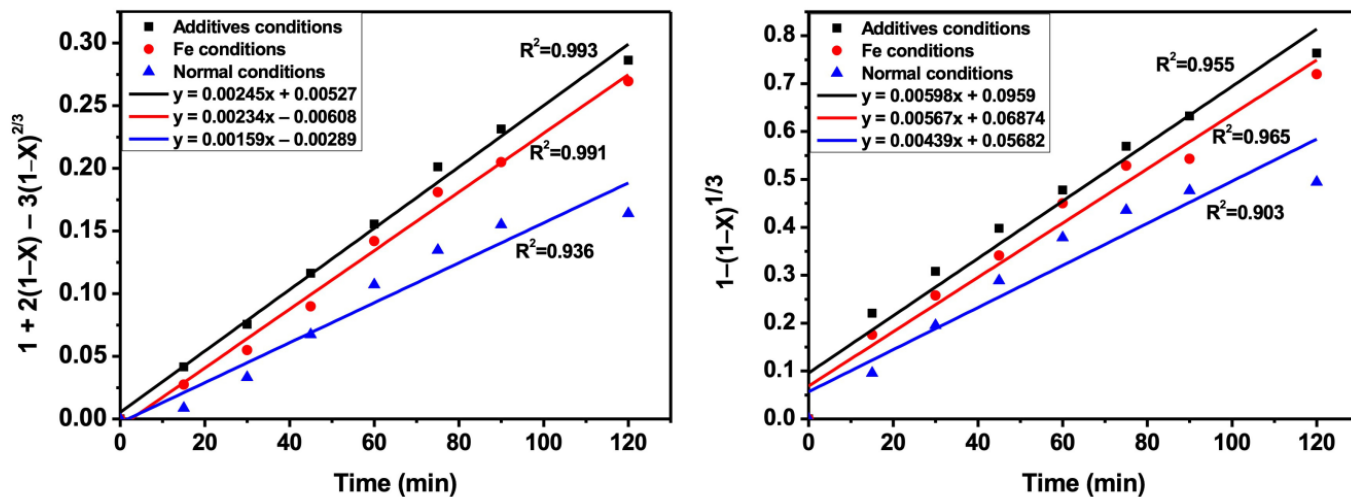


Figure 11. Plot of $1 + 2(1 - x) - 3(1 - x)^{2/3}$ vs. time (left) and $1 - (1 - x)^{1/3}$ vs. time (right) under different leaching conditions.

The relation between the overall rate constant, k_1 , obtained from Figure 11 at various temperatures, is described by the Arrhenius Equation (10):

$$k_1 = A \exp\left(\frac{-E_a}{RT}\right) \tag{10}$$

where k_1 is the overall rate constant ($m \cdot min^{-1}$), A is the frequency factor (min^{-1}), E_a is the activation energy ($J \cdot mol^{-1}$), R is the universal gas constant ($8.314 J \cdot K^{-1} \cdot mol^{-1}$), and T is the reaction temperature (K). Plotting the values of $\ln k_1$ obtained at different temperatures against $1/T$ gave a straight line with a correlation coefficient of 0.897 (Figure 12). The calculated activation energy E_a from the slope is 19.13 kJ/mol, which is within the range of the product layer diffusion control reaction model. It has previously been reported that the activation energy of the diffusion controlled reactions is below 20 kJ/mol, while for chemical-controlled reactions is above 40 kJ/mol [42,56]. The calculated E_a value in the current study is comparable to the 17.60 kJ/mol reported by Ramadan et al. [8]. The reported activation energy of 17.60 kJ/mol was achieved with the size fraction of $-63 \mu m$. Therefore, addition of both metallic Fe and $MgSO_4$ significantly enhanced the Fe dissolution rate, yielding the similar effect comparable to small-sized particles. Contrary to the obtained E_a value in current study, higher E_a values (>20 kJ/mol) have been reported for the product layer diffusion model. For example, Sasikumar et al. [24] reported the activation energy of 64 kJ/mol for the Fe dissolution, while Olanipekun [44] and Jabit [57] obtained 62.4 kJ/mol and 90 kJ/mol, respectively. The discrepancy in the E_a value has led to some researchers to conclude that it is better to predict the rate controlling mechanism of the heterogenous dissolution reactions from kinetic equations.

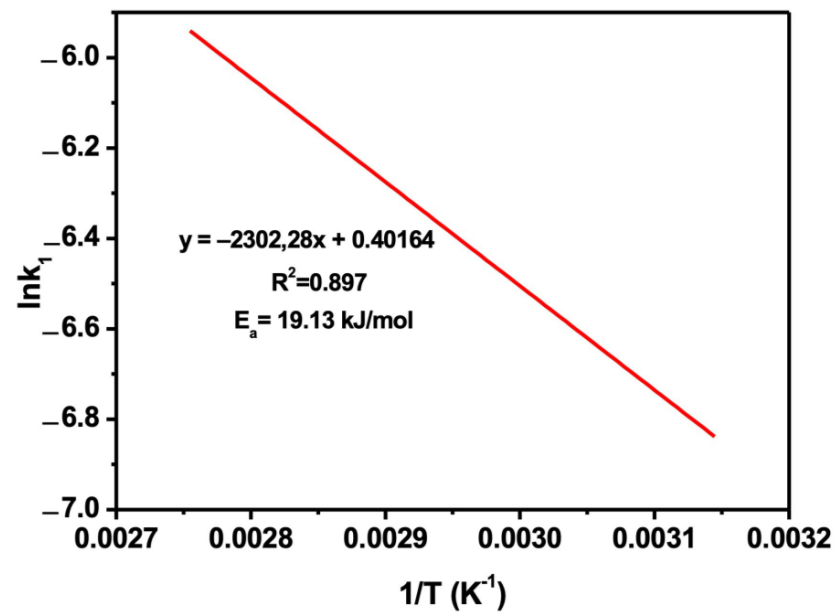


Figure 12. Plot of $\ln k_1$ against $1/T$ for Fe leaching in additives conditions.

3.11. Characterization of the Leach Residue

The undissolved residue produced at the optimum leaching conditions was separated and dried at 120 °C and the morphological analysis was performed. Compared to the as-received ilmenite (Figure 2), the morphology of the leached sample consists of a mixture of irregular-shaped large- and small-sized particles (Figure 13). At higher magnification (Figure 13b,c), it is observed that the small-sized particles form agglomerates on the particle surface. The deposits of solid particles on the surface depicts that the complete Fe dissolution was inhibited, and hence the recovery was below 100%. In addition, this validates that the reaction kinetics of ilmenite is controlled by the product layer diffusion, which is consistent with the results in Figure 11. Further analysis was carried out with EDS to determine elemental composition of the leached residue. EDS results corresponding to the different regions shown in SEM images in Figure 13 are presented in Figure 14. The EDS spectrum (Figure 14) of the overall sample (Figure 13a) illustrate that the leached residue is high in Ti compared to Fe. This verifies that most of the Fe was leached out while the Ti remained undissolved. However, the EDS spectra of regions 1–3 (shown in Figure 13b–d as spectrum 1–3) indicates impurities such as Al, Si, Mg, and Mn, which remained undissolved during the leaching process.

The X-ray diffraction pattern of the dried residue in Figure 15 shows the surfacing of the rutile phase, which is indicative of the transformation of intermediate phases [36]. However, the ilmenite phase is still present in the leached sample, which is verified by presence of elemental Fe, as shown by EDS (Figure 14). In addition, the only impurity phase detected is SiO₂, conflicting the EDS results (Figure 14). This suggests that other impurities are available in trace amounts, as they were not detected by XRD. Chemical composition (Table 5) confirmed that the leached residue was comprised of 91.4% rutile TiO₂, which is comparable to the 90% reported by Mahmoud et al. [9] on the calcined residue obtained at optimum leaching conditions (HCl stoichiometry: 1.2; HCl concentration: 20%; solid/liquid: 1/7.23 g/g; temperature: 110 °C; Fe addition time: 30 min; Fe stoichiometry: 1:1). The dominant rutile phase illustrates that the leached residue can be used as a feed for synthetic rutile production. The additional phases in high content are ilmenite FeTiO₃ (4.37%) and SiO₂ (2.23%), while Al₂O₃, MgO, MnO₂, CaO, V₂O₅, MnO₂, and Cr₂O₃ were below 0.13%. However, the detected SiO₂ impurity in the leached residue means that a purification process will be required to improve the quality of the synthetic rutile [9]. The low levels of V₂O₅, MnO₂, and Cr₂O₃ indicate that the residue is suitable for use in the production

of white pigments by chlorination [9]. The hydrometallurgical flowsheet describing Fe extraction from the ilmenite ore with HCl acid in the presence of metallic Fe and MgSO₄ additive is presented in Figure 16.

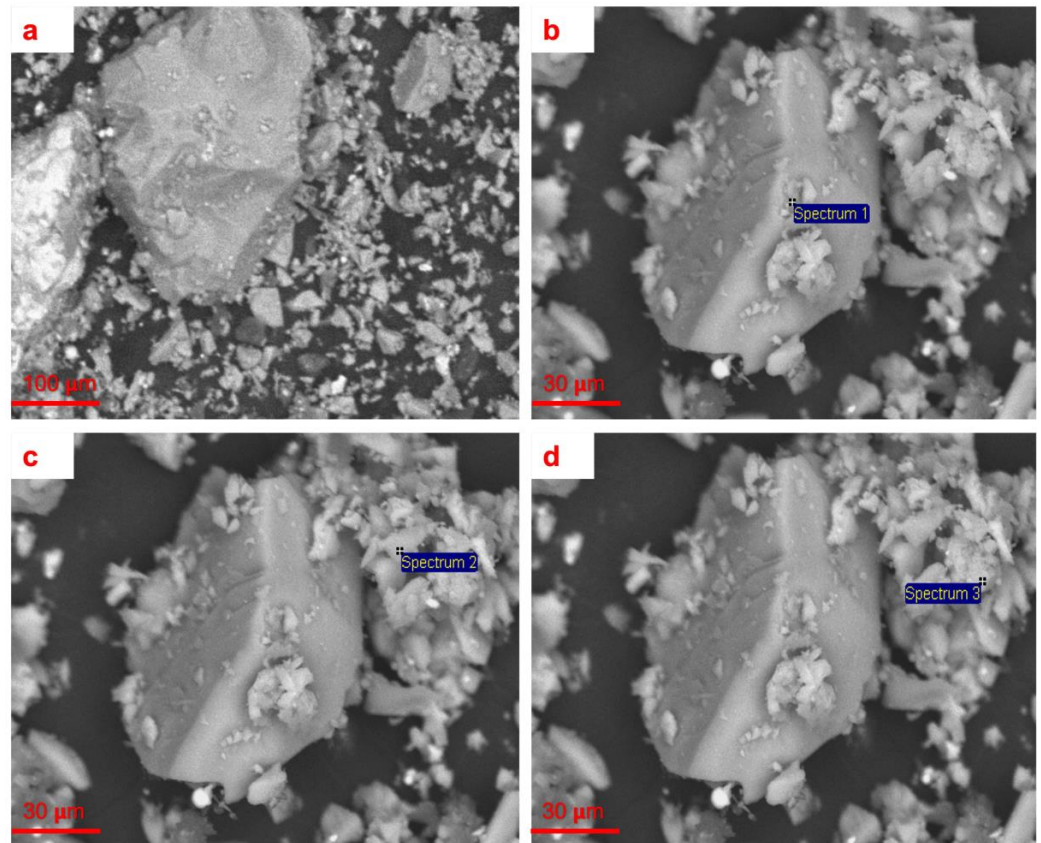


Figure 13. SEM images of the leached residue under additives conditions at (a) low magnification and (b–d) high magnification after 120 min.

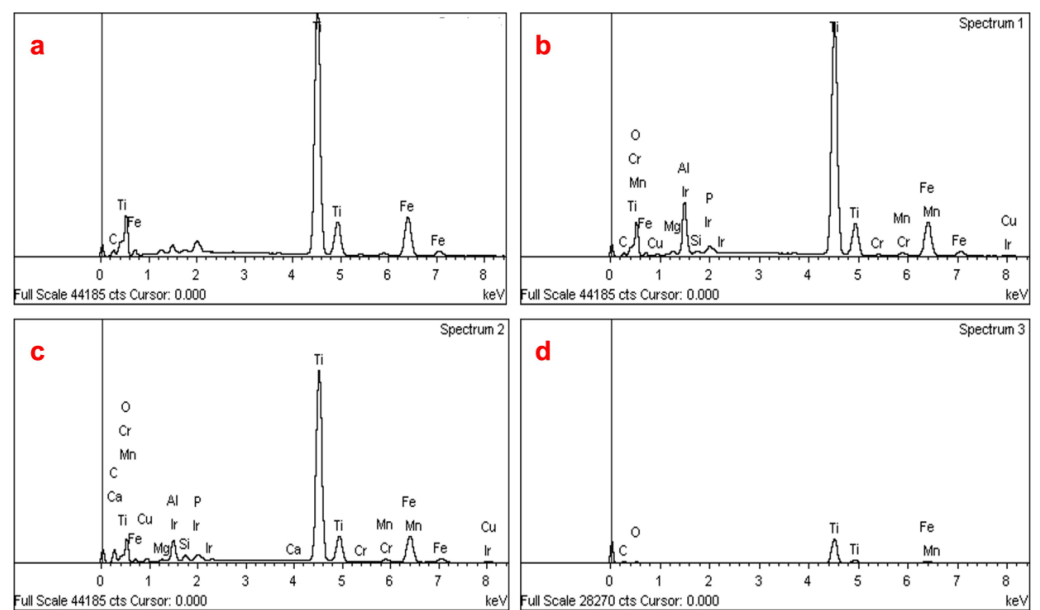


Figure 14. EDS analysis of the solid residue at (a) low magnification and (b–d) high magnification.

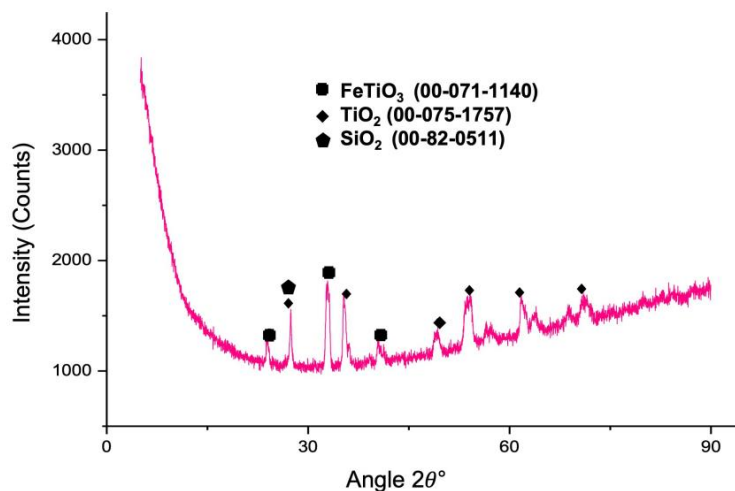


Figure 15. XRD pattern of the leached residue under optimum leaching conditions.

Table 5. Chemical composition (wt.%) of the leached residue obtained by XRF.

Chemical Composition	wt.%
TiO ₂	91.4
FeTiO ₃	4.37
SiO ₂	2.23
Al ₂ O ₃	0.09
CaO	0.01
MnO ₂	0.03
MgO	0.06
Cr ₂ O ₃	0.01
V ₂ O ₅	0.13
LOI	1.67

LOI = loss on ignition.

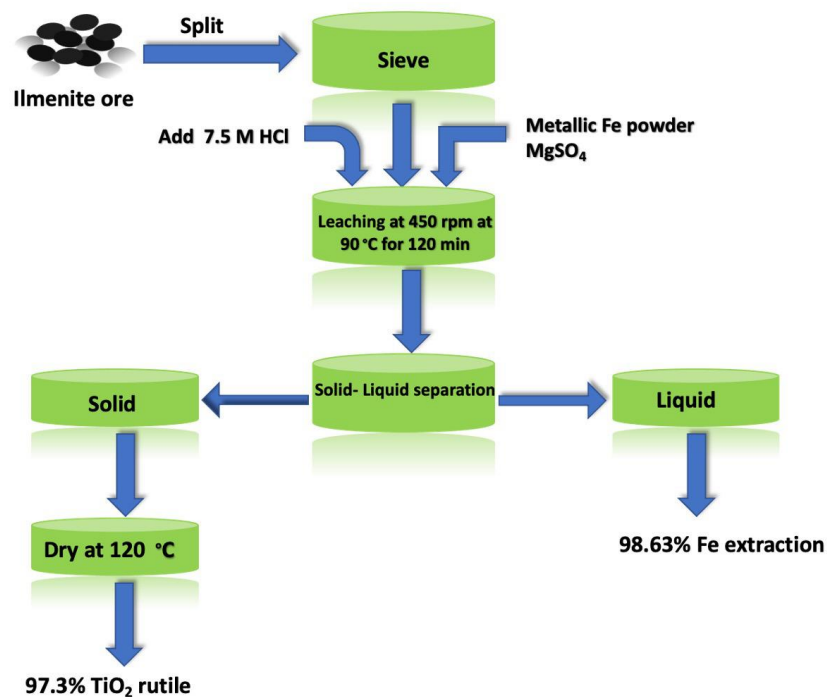


Figure 16. Schematic flow diagram of Fe leaching from ilmenite by HCl acid in the presence of metallic Fe and MgSO₄ additive.

4. Conclusions

This paper investigated the direct leaching of ilmenite ore in HCl to establish the dissolution of iron. The primary parameters, such as acid concentration, particle size distribution, temperature, ilmenite and acid ratio, agitation rate, and leaching time were studied to optimize the leaching conditions. From the experiments, the results can be summarized as follows:

Mineralogical analysis of the as-received ilmenite concentrate showed that the diverse grain morphology consisted mainly of an ilmenite and rutile phase with traces of impurities, as detected by EDS and XRF measurements. Ilmenite ore with large-sized particles of +150 μm exhibited high leaching efficiency compared to small-sized particles ($-75 \mu\text{m}$) when a high acid concentration of 7.5 M was utilized. Increasing the agitation speed from 350 to 450 rpm resulted in an Fe extraction of 92.32% accompanied by a 2.40% Ti loss in the solution. A high solid–acid ratio (3:20) yielded a slow polymerization reaction, yielding low efficiency. The addition of metallic Fe powder at low solid–acid ratios enhanced the leachability of the iron. The inclusion of MgSO_4 was more effective in contrast to Na_3PO_4 and NaF additives, providing a superior catalytic effect. The Fe extraction of 98.63% was attained after 120 min under the Fe- MgSO_4 -HCl condition, indicating the significance of a prolonged leaching time. The Ti recovery on the leached residue was 97.3%. The XRF measurements confirmed that Ti remained undissolved during the leaching process, as a TiO_2 content of about 91.4% was detected on the solid residue. Furthermore, this showed that the leached residue can be used as feed in the manufacturing of synthetic rutile. Moreover, a high content of impurities such as ilmenite FeTiO_3 (4.37%) and SiO_2 (2.23%) were observed along with traces of Al_2O_3 , MgO , MnO_2 , CaO , V_2O_5 , MnO_2 , and Cr_2O_3 impurities. However, to achieve a high-quality rutile product, a purification process will be required to decrease the SiO_2 content. The leaching kinetics of the Fe dissolution in HCl was found to conform to the shrinking core model, where the product layer diffusion is rate-controlling, with an apparent activation energy of 19.13 kJ/mol.

Supplementary Materials: The following supporting information can be downloaded at: <https://www.mdpi.com/article/10.3390/min12101336/s1>, Figure S1. The concentration of the dissolved metal ions in an aqua regia solution with (a,b) 10 mL HNO_3 30 mL HCl and (c,d) 20 mL HNO_3 60 mL HCl.

Author Contributions: Conceptualization and methodology, M.M.R.; investigation, K.D.; data curation, N.N.; writing—original draft preparation, K.D. and N.N.; writing—review and editing, T.M., M.M.R., and M.B.S.; supervision, M.M.R. and M.B.S. All authors have read and agreed to the published version of the manuscript.

Funding: This research was funded by South African National Research Foundation (NRF) Thuthuka, grant number 13891.

Acknowledgments: The authors would like to give thanks to the Institute of Nano-Engineering Research, and the Tshwane University of Technology for XRD, SEM, and ICP analysis. The support of the CSIR organization is gratefully appreciated.

Conflicts of Interest: The authors declare no conflict of interest. The funders had no role in the design of the study; in the collection, analyses, or interpretation of data; in the writing of the manuscript; or in the decision to publish the results.

References

1. Juergen, H.; Braun, A.; Baidins, R.; Marganski, E. TiO_2 Pigment Technology: A Review. *Prog. Org. Coat.* **1992**, *20*, 109–110.
2. He, Y.; Sutton, N.B.; Rijnaarts, H.H.M.; Langenhoff, A.A.M. Corrigendum to “Degradation of Pharmaceuticals in Wastewater Using Immobilized TiO_2 Photocatalysis under Simulated Solar Irradiation” [Appl. Catal. B: Environ. 182 (2016) 132–141]. *Appl. Catal. B Environ.* **2016**, *189*, 283. [[CrossRef](#)]
3. Yadav, S.C.; Sharma, A.; Devan, R.S.; Shirage, P.M. Role of Different Counter Electrodes on Performance of TiO_2 Based Dye-Sensitized Solar Cell (DSSC) Fabricated with Dye Extracted from Hibiscus Sabdariffa as Sensitizer. *Opt. Mater.* **2022**, *124*, 112066. [[CrossRef](#)]
4. Song, T.; Paik, U. TiO_2 as an Active or Supplemental Material for Lithium Batteries. *J. Mater. Chem. A* **2016**, *4*, 14–31. [[CrossRef](#)]

5. Samal, S. The Dissolution of Iron in the Hydrochloric Acid Leach of Titania Slag Obtained from Plasma Melt Separation of Metalized Ilmenite. *Chem. Eng. Res. Des.* **2011**, *89*, 2190–2193. [[CrossRef](#)]
6. Thambiliyagodage, C.; Wijesekera, R.; Bakker, M.G. Leaching of Ilmenite to Produce Titanium Based Materials: A Review. *Discov. Mater.* **2021**, *1*, 1–28. [[CrossRef](#)]
7. Shahien, M.G.; Khedr, M.M.H.; Maurice, A.E.; Farghali, A.A.; Ali, R.A.M. Synthesis of High Purity Rutile Nanoparticles from Medium-Grade Egyptian Natural Ilmenite. *Beni-Suef Univ. J. Basic Appl. Sci.* **2015**, *4*, 207–213. [[CrossRef](#)]
8. Ramadan, A.M.; Farghaly, M.; Fathy, W.M.; Ahmed, M.M. Leaching and Kinetics Studies on Processing of Abu-Ghalaga Ilmenite Ore. *Int. Res. J. Eng. Technol.* **2016**, *3*, 46–53.
9. Mahmoud, M.H.H.; Afifi, A.A.I.; Ibrahim, I.A. Reductive Leaching of Ilmenite Ore in Hydrochloric Acid for Preparation of Synthetic Rutile. *Hydrometallurgy* **2004**, *73*, 99–109. [[CrossRef](#)]
10. Grey, I.; MacRae, C.; Silvester, E.; Susini, J. Behaviour of Impurity Elements during the Weathering of Ilmenite. *Mineral. Mag.* **2005**, *69*, 437–446. [[CrossRef](#)]
11. Wang, Y.; Yuan, Z.; Matsuura, H.; Tsukihashi, F. Reduction Extraction Kinetics of Titania and Iron from an Ilmenite by H₂-Ar Gas Mixtures. *ISIJ Int.* **2009**, *49*, 164–170. [[CrossRef](#)]
12. Akhgar, B.N.; Pazouki, M.; Ranjbar, M.; Hosseinnia, A.; Salarian, R. Application of Taguchi Method for Optimization of Synthetic Rutile Nano Powder Preparation from Ilmenite Concentrate. *Chem. Eng. Res. Des.* **2012**, *90*, 220–228. [[CrossRef](#)]
13. Manhique, A.J.; Focke, W.W.; Madivate, C. Titania Recovery from Low-Grade Titaniferous Minerals. *Hydrometallurgy* **2011**, *109*, 230–236. [[CrossRef](#)]
14. Demeri, M.Y.; Kipouros, G.J. Processing Titanium and Lithium for Reduced-Cost Application. *JOM* **1997**, *49*, 20. [[CrossRef](#)]
15. Zhang, W.; Zhu, Z.; Cheng, C.Y. A Literature Review of Titanium Metallurgical Processes. *Hydrometallurgy* **2011**, *108*, 177–188. [[CrossRef](#)]
16. Liu, Y.; Qi, T.; Chu, J.; Tong, Q.; Zhang, Y. Decomposition of Ilmenite by Concentrated KOH Solution under Atmospheric Pressure. *Int. J. Miner. Process.* **2006**, *81*, 79–84. [[CrossRef](#)]
17. Van Vuuren, D.S. A Critical Evaluation of Processes to Produce Primary Titanium. *J. S. Afr. Inst. Min. Metall.* **2009**, *109*, 455–461.
18. Habashi, F.; Kamaledine, F.; Bourricaudy, E. A New Process to Upgrade Ilmenite to Synthetic Rutile. *Metall* **2015**, *69*, 27–30.
19. Ogasawara, T.; de Araújo, R.V.V. Hydrochloric Acid Leaching of a Pre-Reduced Brazilian Ilmenite Concentrate in an Autoclave. *Hydrometallurgy* **2000**, *56*, 203–216. [[CrossRef](#)]
20. Mostafa, N.Y.; Hessien, M.M.; Shaltout, A.A. Hydrothermal Synthesis and Characterizations of Ti Substituted Mn-Ferrites. *J. Alloys Compd.* **2012**, *529*, 29–33. [[CrossRef](#)]
21. Demopoulos, G.P.; Li, Z.; Becze, L.; Moldoveanu, G.; Cheng, T.C.; Harris, B. New Technologies for HCl Regeneration in Chloride Hydrometallurgy. *World Metall.* **2008**, *61*, 89–98.
22. De, A.K.; Khopkar, S.M.; Chalmers, R.A. *Solvent Extraction of Metals*; Ven Nostrand, Reinhold Co.: London, UK, 1970.
23. Tanaka, M. *Chemistry of Solvent Extraction*; Kyoritsu Shuppan: Tokyo, Japan, 1977; pp. 2–38.
24. Sasikumar, C.; Rao, D.S.; Srikanth, S.; Mukhopadhyay, N.K.; Mehrotra, S.P. Dissolution Studies of Mechanically Activated Manavalakurichi Ilmenite with HCl and H₂SO₄. *Hydrometallurgy* **2007**, *88*, 154–169. [[CrossRef](#)]
25. Mackey, T.S. Acid Leaching of Ilmenite into Synthetic Rutile. *Ind. Eng. Chem. Prod. Res. Dev.* **1974**, *13*, 9–18. [[CrossRef](#)]
26. Tao, T.; Chen, Q.Y.; Hu, H.P.; Yin, Z.L.; Chen, Y. TiO₂ Nanoparticles Prepared by Hydrochloric Acid Leaching of Mechanically Activated and Carbothermic Reduced Ilmenite. *Trans. Nonferrous Met. Soc. China Engl. Ed.* **2012**, *22*, 1232–1238. [[CrossRef](#)]
27. Wei, L.; Hu, H.; Chen, Q.; Tan, J. Effects of Mechanical Activation on the HCl Leaching Behavior of Plagioclase, Ilmenite and Their Mixtures. *Hydrometallurgy* **2009**, *99*, 39–44. [[CrossRef](#)]
28. Duncan, J.; Metson, J. Acid Attack on New Zealand Ilmenite. I: The Mechanism of Dissolution. II: The Structure and Composition of the Solid. *N.Z.J. Sci.* **1982**, *25*, 111–116.
29. Sasikumar, C.; Rao, D.S.; Srikanth, S.; Ravikumar, B.; Mukhopadhyay, N.K.; Mehrotra, S.P. Effect of Mechanical Activation on the Kinetics of Sulfuric Acid Leaching of Beach Sand Ilmenite from Orissa, India. *Hydrometallurgy* **2004**, *75*, 189–204. [[CrossRef](#)]
30. Tkáčová, K.; Baláž, P. Reactivity of Mechanically Activated Chalcopyrite. *Int. J. Miner. Process.* **1996**, *44*, 197–208. [[CrossRef](#)]
31. Welham, N.J. Enhanced Dissolution of Tantalite/Columbite Following Milling. *Int. J. Miner. Process.* **2001**, *61*, 145–154. [[CrossRef](#)]
32. Das, G.K.; Pranolo, Y.; Zhu, Z.; Cheng, C.Y. Leaching of Ilmenite Ores by Acidic Chloride Solutions. *Hydrometallurgy* **2013**, *133*, 94–99. [[CrossRef](#)]
33. Gireesh, V.S.; Vinod, V.P.; Nair, S.K.; Ninan, G. Effect of Sulphate Ions on Leaching of Ilmenite with Hydrochloric Acid. *J. Acad. Ind. Res.* **2013**, *2*, 402–404.
34. Habib, M.A.; Biswas, R.K.; Ali, M.R.; Hasan, A.K.M. Leaching of Non-Treated Ilmenite by HCl-CH₃OH-H₂O Mixture and Its Kinetics. *Indian J. Chem. Technol.* **2006**, *13*, 53–59.
35. Janssen, A.; Putnis, A. Processes of Oxidation and HCl-Leaching of Tellnes Ilmenite. *Hydrometallurgy* **2011**, *109*, 194–201. [[CrossRef](#)]
36. Ramakokovhu, M.; Ramakokovhu, M.M.; Olubambi, P.A.; Mbaya, R.K.K.; Mojisola, T.; Teffo, M.L. Mineralogical and Leaching Characteristics of Altered Ilmenite Beach Placer Sands. *Minerals* **2020**, *10*, 1022. [[CrossRef](#)]
37. Mojisola, T.; Ramakokovhu, M.M.; Raethel, J.; Olubambi, P.A.; Matizamhuka, W.R. In-Situ Synthesis and Characterization of Fe-TiC Based Cermet Produced from Enhanced Carbothermally Reduced Ilmenite. *Int. J. Refract. Met. Hard Mater.* **2019**, *78*, 92–99. [[CrossRef](#)]

38. Klepka, M.; Lawniczak-Jablonska, K.; Jablonski, M.; Wolska, A.; Minikayev, R.; Paszkowicz, W.; Przepiera, A.; Spolnik, Z.; Grieken, R. Van Combined XRD, EPMA and X-Ray Absorption Study of Mineral Ilmenite Used in Pigments Production. *J. Alloys Compd.* **2005**, *401*, 281–288. [[CrossRef](#)]
39. Nayl, A.A.; Awwad, N.S.; Aly, H.F. Kinetics of Acid Leaching of Ilmenite Decomposed by KOH. Part 2. Leaching by H₂SO₄ and C₂H₂O₄. *J. Hazard. Mater.* **2009**, *168*, 793–799. [[CrossRef](#)]
40. Haverkamp, R.G.; Kruger, D.; Rajashekar, R. The Digestion of New Zealand Ilmenite by Hydrochloric Acid. *Hydrometallurgy* **2016**, *163*, 198–203. [[CrossRef](#)]
41. Vilakazi, A.Q. Hydrometallurgical Beneficiation of Ilmenite. Master's Thesis, University of the Free State, Bloemfontein, South Africa, 2017.
42. Contreras, M.; Gazquez, J.; Bolivar, J.P. Isolation and Characterization of the Mineral Phases in Ilmenite Ore: Optimization of the TiO₂ Pigment Process Abstract. *J. Waste Recycl.* **2017**, *2*, 1–9.
43. Hugo, V.E. A Study of Titanium-Bearing Oxides in Heavy Mineral Deposits along the East Coast of South Africa. Ph.D. Thesis, University of Natal, Durban, South Africa, 1993.
44. Olanipekun, E. A Kinetic Study of the Leaching of a Nigerian Ilmenite Ore by Hydrochloric Acid. *Hydrometallurgy* **1999**, *53*, 1–10. [[CrossRef](#)]
45. Baba, A.A.; Swaroopa, S.; Ghosh, M.K.; Adekola, F.A. Mineralogical Characterization and Leaching Behavior of Nigerian Ilmenite Ore. *Trans. Nonferrous Met. Soc. China Engl. Ed.* **2013**, *23*, 2743–2750. [[CrossRef](#)]
46. Jabit, N.A. Chemical and Electrochemical Leaching Studies of Synthetic and Natural Ilmenite in Hydrochloric Acid Solutions. Ph.D. Thesis, Murdoch University, Perth, Australia, 2017; pp. 1–303.
47. Deysel, K. Leucoxene Study: A Mineral Liberation Analysis (MLA) Investigation. In Proceedings of the the 6th International Heavy Minerals Conference 'Back to Basics', Hluhluwe, South Africa, 9–14 September 2007; pp. 167–172.
48. Jackson, J.S. *A Kinetic Study of the Dissolution of Allard Lake Ilmenite in Hydrochloric Acid*; The University of Utah: Salt Lake City, UT, USA, 1975; ISBN 9798660719035.
49. Sinha, H.N. Hydrochloric Acid Leaching of Ilmenite. In Proceedings of the Symposium on Extractive Metallurgy, Australian Institute of Mining and Metallurgy, Melbourne, Australia, 12–14 November 1984; pp. 163–168.
50. Zheng, T.; Li, J.-J.; Wang, L.-L.; Wang, Z.-J.; Wang, J.-C. Implementing Continuous Freeze-Casting by Separated Control of Thermal Gradient and Solidification Rate. *Int. J. Heat Mass Transf.* **2019**, *133*, 986–993. [[CrossRef](#)]
51. Van Dyk, J.P.; Vegter, N.M.; Pistorius, P.C. Kinetics of Ilmenite Dissolution in Hydrochloric Acid. *Hydrometallurgy* **2002**, *65*, 31–36. [[CrossRef](#)]
52. Lu, Z.-Y.; Muir, D.M. Dissolution of Metal Ferrites and Iron Oxides by HCl under Oxidising and Reducing Conditions. *Hydrometallurgy* **1988**, *21*, 9–21. [[CrossRef](#)]
53. Reid, A.F.; Sinha, H.N.; Commonwealth Scientific and Industrial Research Organization. Treatment of Ilmenite. U.S. Patent US3922164A, 25 November 1975.
54. Dubenko, A.; Nikolenko, M.; Kostyniuk, A.; Likozar, B. Sulfuric Acid Leaching of Altered Ilmenite Using Thermal, Mechanical and Chemical Activation. *Minerals* **2020**, *10*, 538. [[CrossRef](#)]
55. Levenspiel, O. *Chemical Reaction Engineering*; John Wiley & Sons: Hoboken, NJ, USA, 1998; ISBN 047125424X.
56. Crundwell, F.K. The Dissolution and Leaching of Minerals: Mechanisms, Myths and Misunderstandings. *Hydrometallurgy* **2013**, *139*, 132–148. [[CrossRef](#)]
57. Jabit, N.A.; Senanayake, G. Characterization and Leaching Kinetics of Ilmenite in Hydrochloric Acid Solution for Titanium Dioxide Production. *J. Phys. Conf. Ser.* **2018**, *1082*, 012089. [[CrossRef](#)]